Trends in the Spectral and Redox Potential Data of Mononuclear Iron(III) ($S = \frac{5}{2}$) Phenolate Complexes

Krishnamoorthi Ramesh and Rabindranath Mukherjee *
Department of Chemistry, Indian Institute of Technology, Kanpur 208 016, India

A series of high-spin octahedral iron(III) complexes of Schiff bases derived from salicylaldehyde and aromatic amines has been synthesised. The ligands were selected to encompass various co-ordination spheres FeN_2O_4, $FeN_2O_2O'_2$, FeN_3O_3 and FeN_4O_2 (where O represents a phenolic oxygen, N an aliphatic or aromatic nitrogen and O' a carboxylate oxygen) to provide generalizations regarding the overall co-ordination environment of the iron centre in a closely related group of complexes. They reveal the effect of stereochemical and/or donor atom variations on the UV/VIS and EPR spectra and Fe^{III}–Fe^{II} redox potentials. Information on the iron(III) site symmetry has been obtained by EPR measurements. The optical spectra are largely determined by transitions originating in the iron–salicylaldiminate chromophore. The ligand-to-metal charge-transfer bands systematically shift to higher energy as the number of phenolate-containing donor sites increases. This blue shift is also reflected in more negative Fe^{III}–Fe^{II} redox potentials. The order of increasing cathodic potential shift with respect to the co-ordination sphere is $N_2O_4 > N_2O_2O'_2 > N_3O_3 > N_4O_2$. This is a reflection of the decreased Lewis acidity of the iron(III) centre due to the increase in basicity of the donor atom. A linear spectroelectrochemical correlation has been obtained between the phenolate-to-iron(III) charge-transfer band energy and the Fe^{III}–Fe^{II} redox potential. Based on this correlation, trends in the redox potentials of iron tyrosinate proteins are discussed.

There has been much interest in the structure–function relationships of the iron tyrosinate proteins.[1–5] Extended X-ray absorption fine structure (EXAFS) and three-dimensional X-ray crystallographic studies indicate that the metal is bound to the protein backbone primarily by N and O donor atoms of amino acid side chains, *viz.* aspartate, histidine and tyrosinate. The enzymatic activity of these proteins is considered[5] to be intimately related to their ease of reduction, which in turn is connected to their iron co-ordination environment. Many model compound studies[6,7] have been made to gain insight into the co-ordination environment of the iron centre; however, there have been few systematic studies on the sensitivity of Fe^{III}–Fe^{II} redox potentials to variations of ligand donor atom types in high-spin iron(III) complexes.[7c] Even in their elegant work to model iron tyrosinate proteins, Que and co-workers[7c] utilized [Fe(salen)X] series [H_2salen = *N*,*N*′-ethylenebis(salicylideneimine); X = I, Br, Cl, $MeCO_2$, PhS, PhO, phenanthrene-9,10-diolate(2−) or 3,5-di-*tert*-butylcatecholate(2−)] with built-in constraints on ligand donor atom variation.

The iron complexes of Schiff bases,[8] owing to the ease and flexibility of ligand design, provide an excellent opportunity to observe relatively subtle effects which have received only sporadic attention.[7a–c,g,h,9,10] The purpose of this study is three-fold. First, to prepare a group of mononuclear high-spin six-co-ordinate iron(III) phenolate complexes utilizing simple but systematically modified Schiff-base ligands incorporating the type of donor atoms that mimic the amino acid residues in iron tyrosinate proteins. Secondly, to reveal the effect of ligand donor atom types on the spectral and redox potential data. Thirdly, to provide a meaningful correlation between the phenolate-to-iron(III) charge-transfer band energies and the Fe^{III}–Fe^{II} redox potentials of synthetic iron(III) phenolate complexes having grossly similar stereochemistry and spin state of the metal centre. This would provide further information pertinent to a better understanding of the structure–function relationships of the iron tyrosinate protein active sites. Additionally, very recently Lever[11] has pointed out that, for the six-co-ordinate high-spin iron complexes, the Fe^{III}–Fe^{II} redox potential data base is rather restricted. We find this really surprising. Our endeavour in this area is set against this background.

Experimental

Chemicals and Starting Materials.—Solvents and reagents were obtained from commercial sources and used without further purification unless otherwise stated. Acetonitrile was dried by distillation over CaH_2. For electrochemical experiments (see below) further purification was achieved by treatment with $KMnO_4$–Li_2CO_3[12] followed by distillation over P_4O_{10}. Dimethylformamide (dmf) was purified as before.[13] Ethanol and methanol were distilled from $Mg(OEt)_2$ and $Mg(OMe)_2$, respectively. Diethyl ether was dried first with anhydrous $CaCl_2$ and then refluxed with, and stored over, sodium. Histamine free base (1*H*-imidazole-4-ethanamine) was obtained from histamine dihydrochloride (Aldrich Chemical) by the addition of purified (distilled over KOH) NEt_3. *o*-Hydroxybenzylamine was prepared by the published procedure.[14] Tetrabutylammonium perchlorate was prepared as described previously.[13]

Measurements.—IR spectra were recorded in KBr discs with a Perkin-Elmer M-580 spectrophotometer, electronic spectra with a Perkin-Elmer Lambda-2 spectrophotometer, and ^{1}H NMR spectra in $CDCl_3$–$(CD_3)_2SO$ solutions using a JEOL PMX-60 (60 MHz) or Brüker WP-80 (80 MHz) spectrometer. Solution magnetic susceptibility measurements were made by the usual NMR method[15] with a JEOL PMX-60 (60 MHz) or Bruker WP-80 (80 MHz) spectrometer and made use of the paramagnetic shift of the methyl protons of dmf–MeCN and the $SiMe_4$ reference as the measured NMR parameter. Solvent susceptibilities[16a] and diamagnetic corrections[16b] were taken from literature tabulations. X-Band EPR spectra were recorded with a Varian E-109 C spectrometer fitted with a quartz Dewar for measurements at 77 K (liquid dinitrogen). The spectra were

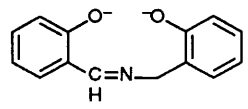

o-N-Salicylideneaminomethylphenolate(2–)
salamp

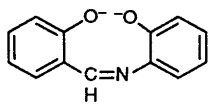

o-N-Salicylideneaminophenolate(2–)
salap

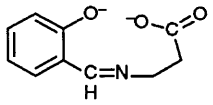

N-Salicylidenealaninate(2–)
salala

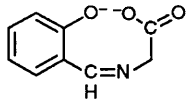

N-Salicylideneglycinate(2–)
salgly

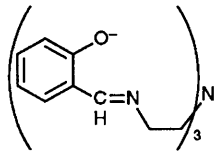

Tris(2-*N*-salicylideneaminoethyl)amine trianion
saltren

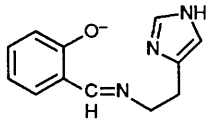

4-(2-*N*-Salicylideneaminoethyl)imidazolate(1–)
salaim

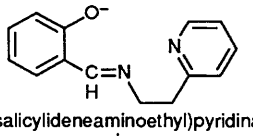

2-(2-*N*-salicylideneaminoethyl)pyridinate(1–)
salapy

calibrated with diphenylpicrylhydrazyl (dpph) (g = 2.0037). Solution electrical conductivity measurements were made with an Elico (Hyderabad, India) type CM-82 T conductivity bridge.

Cyclic voltammetric measurements were performed by using a PAR model 370-4 electrochemistry system incorporating the following: model 174A polarographic analyser; model 175 universal programmer; model RE 0074 *x-y* recorder. Potentials are reported at ≈25 °C relative to an aqueous saturated calomel reference electrode (SCE) and are uncorrected for junction potentials. The solutions were ≈1.0 × 10^{-3} mol dm^{-3} in complex and 0.2 mol dm^{-3} in supporting electrolyte, $NBu^n_4ClO_4$. In acetonitrile and dmf solutions at a scan rate of 50 mV s^{-1} the above condition was found to give the best performance with platinum and glassy carbon electrodes for the $[Fe(\eta\text{-}C_5H_5)_2]^+$–$[Fe(\eta\text{-}C_5H_5)_2]$ couple. At a platinum electrode the E_{298}° and the peak-to-peak separation (ΔE_p) are: dmf, 0.49 (80); MeCN, 0.40 (80 mV). A PAR G0021 glassy carbon electrode or a planar platinum-inlay electrode (Beckman model 39273) was used as the working electrode. The details of the cell configuration are as described before.[13]

Syntheses of Ligands.—The ligands H_2salamp,[17a] H_2salap,[17b] H_3saltren,[18a] and Hsalapy[19] were prepared according to reported procedures; H_2salala, H_2salgly and Hsalaim were generated *in situ* according to reported procedures.[10a,20,21] The isolated ligands were shown to be pure by their ^{1}H NMR spectra at ambient temperature: H_2salamp, δ[$(CD_3)_2SO$] 4.7 (s, 2 H, CH_2), 6.5–7.5 (m, 8 H, aromatic), 8.4 (s, 1 H, N=CH); H_2salap, δ($CDCl_3$) 7.0–7.7 (m, 8 H, aromatic) and 8.8 (s, 1 H, N=CH); H_3saltren, δ($CDCl_3$) 2.8 (t, 6 H, J 7, NCH_2CH_2), 3.5 (t, 6 H, J 7, NCH_2CH_2), 6.0–7.5 (m, 12 H, aromatic) and 7.8 (s, 3 H, N=CH); Hsalapy, δ($CDCl_3$) 3.1 (t, 2 H, J 6.5, NCH_2CH_2), 3.95 (t, 2 H, J 6.5 Hz, NCH_2CH_2), 6.5–8.5 (m, 7 H, aromatic), 8.2 (s, 1 H, N=CH) and 13.5 (s, 1 H, C_6H_4OH) (Found: C, 73.60; H, 5.30; N, 6.30. Calc. for H_2salamp: C, 74.00; H, 5.75; N, 6.15. Found: C, 73.50; H, 5.20; N, 6.30. Calc. for H_2salap: C, 73.25; H, 5.15, N, 6.55. Found: C, 70.55; H, 6.45; N, 12.00. Calc. for H_3saltren: C, 70.75; H, 6.55; N, 12.25%). It is to be noted that the ligand Hsalapy is a liquid.

Syntheses of Complexes.—The following complexes were synthesised following literature methods: $K[Fe(salap)_2]\cdot 2H_2O$,[6b] $K[Fe(salala)_2]\cdot 0.5H_2O$,[20] $K[Fe(salgly)_2]\cdot 0.5H_2O$,[20] $[Fe(saltren)]\cdot 0.5H_2O$,[18] $[Fe(salaim)_2]PF_6\cdot EtOH$.[21] The details of the synthesis of the iron(III) complex $[Fe(salapy)_2]PF_6\cdot MeOH$ are essentially the same as those described in the literature.[22]

Tetrabutylammonium bis(o-N-*salicylideneaminomethylphenolato*)*ferrate*(III). To an ethanolic solution (20 cm^3) of H_2salamp (0.23 g, 1 mmol) was added a 10% solution (5.2 cm^3) of NBu^n_4OH in methanol–toluene. The mixture was stirred for 15 min and an ethanolic (10 cm^3) solution of anhydrous $FeCl_3$ (80 mg, 0.5 mmol) was added dropwise at 298 K. The resulting mixture was heated to reflux for 1 h and subsequently allowed to cool to room temperature and filtered through a G-4 frit. After evaporation of the red solution using a rotary evaporator (≈328 K) the solid thus obtained was dissolved in hot MeCN (5 cm^3). Cooling in a refrigerator resulted in red needle-shaped crystals, which were filtered off, washed with MeCN–Et_2O (1:4 v/v) and recrystallized from MeCN to afford the pure product which was dried at ≈350 K (yield *ca.* 65%) {Found: C, 71.10; H, 7.60; N, 5.50. Calc. for $[NBu^n_4][Fe(salamp)_2]$: C, 70.60; H, 7.75; N, 5.60. Found: C, 55.95; H, 4.00: N, 4.95. Calc. for $K[Fe(salap)_2]\cdot 2H_2O$: C, 56.40; H, 3.95; N, 5.05. Found: C, 50.05; H, 4.00; N, 5.20. Calc. for $K[Fe(salala)_2]\cdot 0.5H_2O$: C, 49.40; H, 3.90; N, 5.75. Found: C, 47.40; H, 3.40; N, 5.90. Calc. for $K[Fe(salgly)_2]\cdot 0.5H_2O$: C, 47.15; H, 3.30; N, 6.10. Found: C, 62.15; H, 5.05; N, 10.30. Calc. for $[Fe(saltren)]\cdot 0.5H_2O$: C, 62.30; H, 5.40; N, 10.75. Found: C, 46.45; H, 4.70; N, 12.20. Calc. for $[Fe(salaim)_2]PF_6\cdot EtOH$: C, 46.25; H, 4.45; N, 12.45. Found: C, 51.25; H, 4.55; N, 8.40. Calc. for $[Fe(salapy)_2]PF_6\cdot MeOH$: C, 50.95; H, 4.40; N, 8.20%}.

Results and Discussion

Syntheses, Selected Properties and Structure.—The complexes were prepared readily using salicylaldehyde, the appropriate amine and iron(III) salt in ethanol or methanol. The iron(III) complexes were isolated as reddish brown to purplish red

Table 1 Some characterization data

Complex	ν(C=N)[a]/cm^{-1}	Λ_M[b]/Ω^{-1} cm^2 mol^{-1}	μ_{eff}[c]
[NBu$^n_4$][Fe(salamp)$_2$]	1633	50	6.10
K[Fe(salap)$_2$]·2H$_2$O	1605	58	6.01 (5.98)[d]
K[Fe(salala)$_2$]·0.5H$_2$O	1590	55	6.10
K[Fe(salgly)$_2$]·0.5H$_2$O	1600	54	5.94 (5.95)[e]
[Fe(saltren)]·0.5H$_2$O	1600	3	5.97
[Fe(salaim)$_2$]PF$_6$·EtOH	1613	75	5.98 (6.0 ± 0.1)[f]
[Fe(salapy)$_2$]PF$_6$·MeOH[g]	1605	175	5.98 (6.03)[h]

[a] KBr disc; ν(C=N) is sharp and strong. [b] Molar conductivity at 298 K in dmf. [c] Measured in dmf solution (room temperature) using the Evans method.[15] Reported magnetic moments at room temperature are given in parentheses. [d] Ref. 6(*b*). [e] Ref. 20. [f] Ref. 21. [g] Solvent is MeCN. ν(PF$_6$) ≈ 840s (br) cm^{-1}. [h] Ref. 22.

Table 2 X-Band EPR spectral data

Compound	Phase	*T*/K	*g*
[NBu$^n_4$][Fe(salamp)$_2$]	Powder	298	*a*
		77	*a*
	Solution[b]	77	4.238, 4.498, 9.446
K[Fe(salap)$_2$]·2H$_2$O	Powder	298	*a*
		77	*a*
	Solution[b]	77	4.323, 9.839
K[Fe(salala)$_2$]·0.5H$_2$O	Powder	298	4.428
		77	4.334
	Solution[b]	77	3.735, 4.309, 4.956, 9.285
K[Fe(salgly)$_2$]·0.5H$_2$O	Powder	298	*a*
		77	*a*
	Solution[b]	77	4.239, 9.351
[Fe(saltren)]·0.5H$_2$O	Powder	298	4.291
		77	*a*
	Solution[b]	77	4.281
[Fe(salaim)$_2$]PF$_6$·EtOH	Powder	298	3.90
		77	2.404, 3.844
	Solution[b]	77	1.883, 2.247, 4.38, 5.258, 9.128
[Fe(salapy)$_2$]PF$_6$·MeOH	Powder	298	4.001
		77	4.056
	Solution[b]	77	4.205

[a] Very broad and weak signal. [b] In dmf solution ([Fe] = 0.02 mol dm^{-3}).

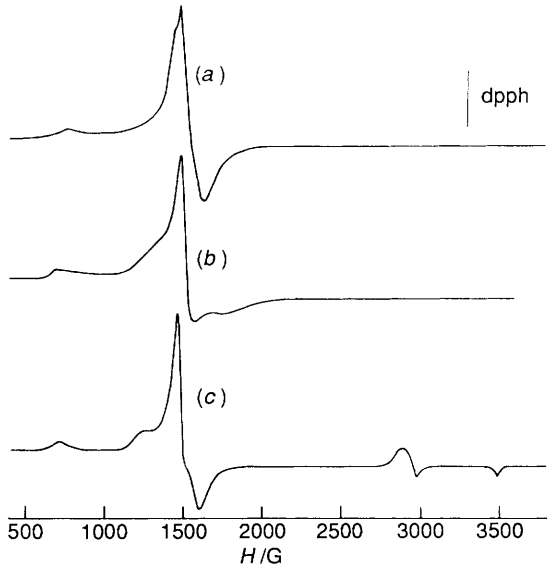

Fig. 1 EPR spectra (X-band) at 77 K: (*a*) [NBu$^n_4$][Fe(salamp)$_2$], (*b*) K[Fe(salala)$_2$]·0.5H$_2$O and (*c*) [Fe(salaim)$_2$]PF$_6$·EtOH in frozen dmf solution; G = 10^{-4} T

crystalline solids. To the best of our knowledge, the synthesis of the complex [NBu$^n_4$][Fe(salamp)$_2$] is reported here for the first time. The purpose behind the choice of the ligand H$_2$-salamp is two-fold. First, the incorporation of a methylene unit into the more familiar conjugated ligand H$_2$salap is expected to disrupt the conjugation between functionalities and allow more flexibility in chelation to the metal ion. Secondly, decreased conjugation in salamp is expected to increase the p_π–p_π* energy gap which might allow one to observe iron(III)-based ligand-field transitions.

A series of iron(III) complexes embracing the co-ordination spheres FeN$_2$O$_4$, FeN$_2$O$_2$O′$_2$, FeN$_3$O$_3$ and FeN$_4$O$_2$ (where O represents a phenolate oxygen, N an aliphatic or aromatic nitrogen and O′ a carboxylate oxygen) has been chosen to provide a systematic variation in the nature of ligand donor atom type to reflect the change in the Lewis acidity of the iron(III) centre in high-spin six-co-ordinate complexes. The ligands chosen are derivatives of salicylaldehyde. Complexes of pertinence to the present investigation are [Fe(salamp)$_2$]$^-$ **1**, [Fe(salap)$_2$]$^-$ **2**, [Fe(salala)$_2$]$^-$ **3**, [Fe(salgly)$_2$]$^-$ **4**, [Fe(saltren)] **5**, [Fe(salaim)$_2$]$^+$ **6** and [Fe(salapy)$_2$]$^+$ **7**.

The imine structure of the ligands is clearly indicated by intense and well resolved ν(C=N) bands near 1600 cm^{-1} in the IR spectra of the complexes. The molar conductances of the anionic/cationic complexes in dmf/MeCN solutions are in the range expected[23] for 1:1 electrolytes. The magnetic moments of the complexes were measured by the Evans method[15] in dmf/MeCN solutions. All six-co-ordinate iron(III) complexes gave values corresponding to a monomeric high-spin d^5 ($S = \frac{5}{2}$) configuration. Selected characterization data for the complexes are given in Table 1. Our data are in excellent agreement with reported values.[6b,18b,20–22]

Quite a few crystal structures of mononuclear six-co-ordinate high-spin iron(III) complexes having phenolate/catecholate, carboxylate and imine/imidazole co-ordination have been determined.[6b,d,7d–f,18b,21,24] The complexes considered here consist of similar or various combinations of the ligand donor atom types present in the reported structures.

EPR Spectra.—In complexes **1**–**7** the overall geometry is octahedral but the environment around the iron(III) centre is varied in a very controlled manner. We thus have a good system to study EPR spectral properties.

The X-band EPR spectra of complexes **1**–**7** were examined for powdered samples at room temperature (298 K) and at 77 K. The signals are very broad and weak. In dmf solution (77 K) the complexes exhibit a well resolved EPR signal near $g = 4.3$ (Fig. 1, Table 2) as predicted for a transition between the middle Kramers doublet of a rhombically distorted high-spin iron(III) complex.[25] It is the most dominant spectral

Table 3 UV/VIS spectral and cyclic voltammetric data

Complex	λ/nm (ε/dm^3 mol^{-1} cm^{-1})[a]	$E_{298}°$/V(ΔE_p/mV)[a,b]
$[NBu^n_4][Fe(salamp)_2]$	329(sh), (16 500), 415 (7700), 982 (2)	−1.41[c]
$K[Fe(salap)_2]\cdot 2H_2O$	296 (30 800), 340(sh), (17 500), 410 (29 700), 490 (10 300), 530(sh) (6600)	−1.26(90)
$K[Fe(salala)_2]\cdot 0.5H_2O$	288 (11 800), 320 (11 000), 421 (3900), 456 (3300)	−0.94(100)
$K[Fe(salgly)_2]\cdot 0.5H_2O$	289 (15 000), 347(sh) (8300), 422 (5000), 460(sh) (4000)	−0.99(70)
$[Fe(saltren)]\cdot 0.5H_2O$	300(sh), (15 000), 325 (17 500), 360(sh), (14 000), 433 (4000), 512 (6450)	−0.81(80)
$[Fe(salaim)_2]PF_6\cdot EtOH$[d]	247 (8100), 330 (10 500), 524 (3800)	−0.44(80)[e]
$[Fe(salapy)_2)PF_6\cdot MeOH$[f]	235 (44 000), 262 (33 900), 327 (10 800), 555 (4700)	−0.22(80)

[a] Solvent is dmf. [b] Meanings of the symbols used as in the text; all potentials are referenced to SCE. Supporting electrolyte is $NBu^n_4ClO_4$ (0.2 mol dm^{-3}), working electrode platinum; scan rate 50 mV s^{-1}. [c] The anodic response is not observed on scan reversal; the $E_{298}°$ value is a rough estimate (cathodic peak potential + 40 mV). [d] The peak at 524 nm shifts to 535 nm in MeCN. [e] In MeCN: −0.47 V (90 mV). [f] Solvent is MeCN. The peak at 555 nm shifts to 532 nm in dmf. In dmf the complex slowly decomposes.

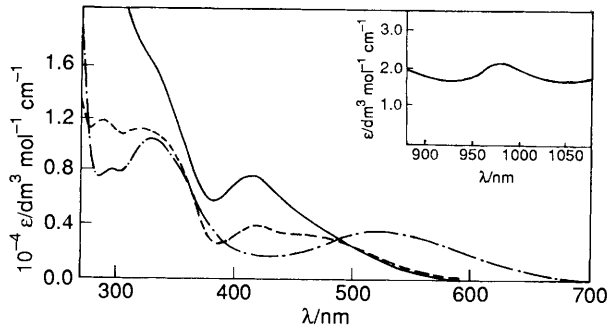

Fig. 2 Absorption spectra of $[NBu^n_4][Fe(salamp)_2]$ (———), $K[Fe(salala)_2]\cdot 0.5H_2O$ (– – –) and $[Fe(salaim)_2]PF_6\cdot EtOH$ (— · — · —) in dmf

feature and is characteristic of near-perfect rhombicity. The weaker resonances at lower fields are due to the ground Kramers doublet of an $S = \frac{5}{2}$ system.

We are somewhat surprised to observe very weak absorptions around $g = 2$ for $[Fe(salaim)_2]^+$ in frozen dmf solution (Fig. 1). Even the powdered sample at 77 K exhibits a signal at $g = 2.404$ (Table 2). Presumably the spectrum in frozen dmf solution is due to the formation of crystallites and subsequent spin–spin interactions. Why we do not see this signal in the room-temperature spectrum of the powdered sample is not clear. The co-ordination polyhedron of the $[Fe(salaim)_2]^+$ cation has a distinct rhombic and a slight tetragonal distortion.[21] The Fe–O distances are 1.917 and 1.910 Å and Fe–N 2.127, 2.138, 2.119 and 2.156 Å. The complex is uniformly high spin as revealed by variable-temperature (4.0–300.0 K) magnetic susceptibility measurements.[21] Additionally, this complex exhibits a paramagnetically shifted ^1H NMR spectrum.[10b]

For complexes **1**, **3** and **6** a splitting in the $g \approx 4.3$ signal is observed (Fig. 1, Table 2). This kind of splitting is observed for the transferrins.[26] The co-ordination environment around the iron(III) centre in $[Fe(salala)_2]^-$ is close to that of the transferrins.[2] Interestingly, $[Fe(salala)_2]^-$ also has optical properties (see below) close to those of an iron(III) transferrin carbonate complex. It is clear that the $g \approx 4.3$ signal is sensitive to the nature of the donor atoms which in turn are related to the changes in the iron environment.

The observed splitting of the $g \approx 4.3$ signal for $[Fe(salala)_2]^-$ demands special attention since Ainscough *et al.*[6b] and McDevitt *et al.*[6f] could not observe such a splitting for their transferrin model complexes.

UV/VIS Spectra.—The absorption spectral results for the complexes are given in Table 3. Representative spectra are displayed in Fig. 2.

The visible absorption spectra are dominated by intense bands in the region 530–410 nm which give rise to the reddish to purplish colours of their solutions. They are assigned to a transition from the p_π orbital of the phenolate oxygen to the half-filled d_{π^*}orbitals of the iron.[6] Thus the spectra are largely determined by electronic transitions originating within the iron salicylaldiminate chromophore. The ligand-to-metal charge-transfer (l.m.c.t.) transitions originating from the carboxylate group are expected to give minor contributions to the near-UV spectrum.[27] Detailed studies on imidazole-to-iron(III) l.m.c.t. transitions are currently limited to low-spin complexes.[28] In $[Fe(salap)_2]^-$ and $[Fe(salgly)_2]^-$ the ligands have one five- and one six-membered chelate ring. In contrast, $[Fe(salamp)_2]^-$, $[Fe(salala)_2]^-$ and $[Fe(salaim)_2]^+/[Fe(salapy)_2]^+$ have two six-membered rings imparting a similar stereochemistry to these complexes.

The following principal aspects emerge from the observations. (*i*) The lowest-energy charge-transfer bands are sensitive to the nature of the co-ordinating atom (Fig. 2, Table 3). The phenolate-to-iron(III) charge-transfer transition shifts to higher energies as the number of phenolates/carboxylates bound to the iron centre increases: $[Fe(salapy)_2]^+/[Fe(salaim)_2]^+$ (FeN_4O_2) < $[Fe(salala)_2]^-$ ($FeN_2O_2O'_2$) < $[Fe(salamp)_2]^-$ (FeN_2O_4). This is a reflection of the decreased Lewis acidity of the iron(III) centre due to the increase in basicity of the donor atom. It is expected to raise the metal d-orbital energies, and hence the gap between the filled phenolate orbitals and the metal t_{2g} orbitals. The present observation is in line with the idea that complexation of Fe^{III} by successive phenolate groups produces a blue shift in the l.m.c.t. transition of about 2000 cm^{-1} per phenolate group.[6a,b,29] (*ii*) In going from $[Fe(salapy)_2]^+/[Fe(salaim)_2]^+$ (FeN_4O_2) to $[Fe(salamp)_2]^-$ (FeN_2O_4) the change in the l.m.c.t. band energy is ≈5300/≈5000 cm^{-1} (Table 3) which is considerably higher than expected. Whereas complexes having the co-ordination sphere FeN_4O_2 carry a positive charge, that having the co-ordination sphere FeN_2O_4 carries a negative charge. Hence, the greater than expected change in energy may be due to the disparate charges on the complexes. The presence of a positive charge may enhance the charge-transfer mechanism in the former complexes. (*iii*) The spectrum of $[Fe(salap)_2]^-$ is more complex than that of $[Fe(salamp)_2]^-$ (Table 3). In $[Fe(salap)_2]^-$ the presence of increased conjugation due to the structure of the ligand reduces the p_π–p_π* energy gap facilitating the charge-transfer transition. Additionally, the free ligand H_2salap is red in contrast to H_2salamp which is yellow similar to most Schiff-base ligands.

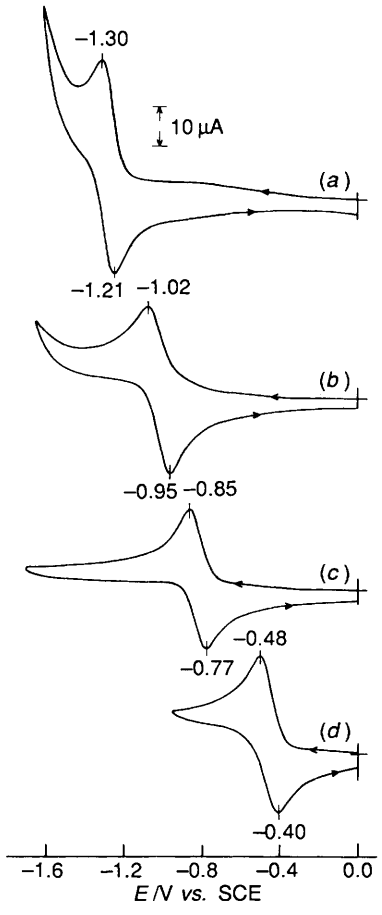

Fig. 3 Cyclic voltammograms (scan rate 50 mV s^{-1}) of (*a*) $K[Fe(salap)_2]\cdot 2H_2O$, (*b*) $K[Fe(salgly)_2]\cdot 0.5H_2O$, (*c*) [Fe(saltren)]·$0.5H_2O$ and (*d*) $[Fe(salaim)_2]PF_6\cdot EtOH$ in dmf at a platinum electrode ([Fe] = 1.0×10^{-3} mol dm^{-3}, 0.2 mol dm^{-3} $NBu^n_4ClO_4$)

(*iv*) In changing the co-ordination sphere from $[Fe(salapy)_2]^+$/$[Fe(salaim)_2]^+$ (FeN_4O_2) to [Fe(saltren)] (FeN_3O_3) the change in charge-transfer energy is only $\approx 730/\approx 450$ cm^{-1} (Table 3) whereas the expected change in this case is $\approx 2650/\approx 2500$ cm^{-1} (see below). It is to be noted that in going from salapy/salaim to saltren the co-ordinating ability of the ligands changes from tri- to hexa-dentate. Additionally, the charge on the complexes $[Fe(salaim)_2]^+$ and $[Fe(salapy)_2]^+$ is unipositive whereas [Fe(saltren)] is neutral. This is expected to increase the l.m.c.t band energy even more, and could be explained by considering better phenolate-to-iron overlap with the saltren ligand, which enforces [18b] an octahedral cage around the central iron(III). (*v*) Keeping the salicylaldimine part of the tridentate ligand fixed, when the other end is changed using two different N-heterocycles as in going from $[Fe(salaim)_2]^+$ to $[Fe(salapy)_2]^+$ in MeCN solution the l.m.c.t. energy decreases by ≈ 670 cm^{-1}. We believe that the factor stabilizing the iron(III) state in the former complex is the base strength [30] of the imidazole (pK = 6.65) relative to that of pyridine (pK = 5.29). (*vi*) The complexes $[Fe(salala)_2]^-$ and $[Fe(salgly)_2]^-$ exhibit l.m.c.t. transitions at ≈ 460 nm. The optical parameters for $[Fe(salala)_2]^-$ (λ_{max} = 456 nm, ε_{Fe} = 3300 dm^3 mol^{-1} cm^{-1}) are very much closer to those of transferrins (λ_{max} = 465 nm, ε_{Fe} = 2600 dm^3 mol^{-1} cm^{-1}). The iron co-ordination environments (site symmetry) of the transferrins and the model compound **3** are closely similar (see above). The present spectral investigation reveals a similar trend in the l.m.c.t. band energy to that observed before.[6b] In this work the comparisons are restricted to a more closely related group of complexes.

The intense l.m.c.t. bands (see above) in the visible region vitiate the observation of ligand-field transitions due to the presence of the high-spin iron(III) centre for most of the complexes **2**–**6**. However, complex **1** displays a very weak broad band at ≈ 980 nm (Fig. 2) assigned [27,31] as the $^6A_1 \longrightarrow {}^4T_1$ (^4G) transition of octahedrally co-ordinated high-spin Fe^{III}. The observation of this band has become possible presumably because of the presence of a l.m.c.t. transition at a very high energy (415 nm) without any low-energy tailing; $[Fe(salamp)_2]^-$ is unique in this regard among iron(III) Schiff-base complexes.

Electrochemistry.—The sensitivity of the Fe^{III}–Fe^{II} redox potential is neatly reflected in the electrochemical behaviour of these complexes when examined by cyclic voltammetry. In dmf solutions at a platinum working electrode a single reversible to quasi-reversible (peak-to-peak separation, ΔE_p, $\approx$ 70–100 mV, $i_{p_c}/i_{p_a} \approx 1$) one-electron process [equation (1)] or the

$$[Fe^{III}L_2]^{-,0,+} + e^- \rightleftharpoons [Fe^{II}L_2]^{2-,-,0} \quad (1)$$

equivalent thereof in the case of **5** is observed (Fig. 3). The formal potentials E_{298}° for the couple (1) were calculated as the average of the cathodic and anodic peak potentials [equation (2)] and are collected in Table 3. They are influenced mainly by

$$E_{298}^\circ = \tfrac{1}{2}(E_{p_c} + E_{p_a}) \quad (2)$$

the ligand electronic properties arising from the donor atom types since the structures of the complexes considered are grossly octahedral; complex **5** is the only odd member. The voltammetric characteristics are practically identical in dmf and in MeCN solutions. The complex $[Fe(salaim)_2]^+$ has been examined in both (Table 3). In dmf–MeCN solutions the cyclic voltammograms of $[Fe(salamp)_2]^-$ are irreversible at platinum and glassy carbon electrodes. This is related to the intrinsic stability of the complex (E_{p_c} −1.41 V) to reduction. The one-electron nature of the redox process (1) in dmf has been identified by comparison of the current height with the redox behaviour of an authentic [13] one-electron reduction system: [Mn(bpb)Cl] [H_2bpb = 1,2-bis(pyridine-2-carboxamido)benzene].

The order of increasing cathodic potential shift with respect to the co-ordination sphere is N_2O_4 (**1** and **2**) > $N_2O_2O'_2$ (**3** and **4**) > N_3O_3 (**5**) > N_4O_2 (**6** and **7**). From the E_{298}° values (Table 3) it becomes evident that the more basic ligands shift the reduction potential to more negative values, whilst the less basic ligands have the opposite effect. Among the complexes **1**–**7**, **1** has the most negative E_{298}°. It is ≈ 150 mV more negative than that of **2** even though both complexes have similar co-ordination spheres (FeN_2O_4) and charge types. The more delocalized nature of the ligand salap compared to salamp reduces the p_π–p_π^* energy gap, rendering its l.m.c.t absorption maximum at a lower energy (see above) and a comparatively more stabilized d* orbital, as is manifested in the E_{298}° value. On passing from the salala to salgly ligand the Fe^{III}–Fe^{II} redox potential becomes more negative (≈ 50 mV). This is attributable to subtle steric constraints in the latter compound. The potential of **6** is more negative (220 mV) than that of **7** due to the change in pK value [30] of the N-heterocycles. A similar effect was observed in the UV/VIS spectra.

Two main results emerge from a closer look into the E_{298}° values of these complexes (Table 3). (*i*) The redox potential for $[Fe(salamp)_2]^-$ (FeN_2O_4) is more negative (470 mV) than those for $[Fe(salala)_2]^-$ ($FeN_2O_2O'_2$). The overall stereochemistry as well as the charge type are invariant. Thus, substitution of two phenolates for two carboxylates lowers the Fe^{III}–Fe^{II} redox potential by 470 mV, *i.e.* a ≈ 230 mV more negative potential shift for introduction of one phenolate group for one carboxylate group. A similar trend was observed in the [Fe(salen)X] series [7c] but the shift was ≈ 110 mV compared to ≈ 230 mV observed here. (*ii*) Comparing the redox potentials

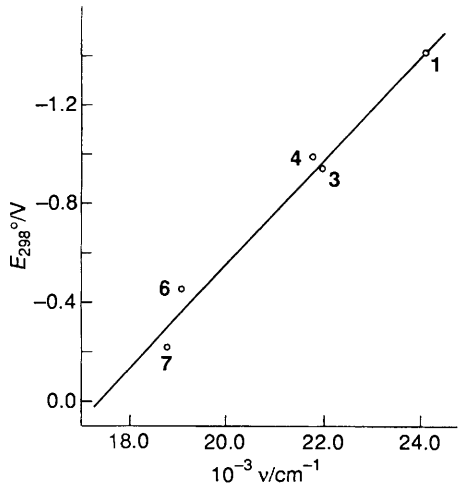

Fig. 4 Correlation of $E_{298}°$ (Fe^{III}–Fe^{II}) with phenolate-to-iron(III) charge-transfer band energy for the complexes **1**, **3**, **4**, **6** and **7**

between $[Fe(salamp)_2]^-$ (FeN_2O_4) and $[Fe(salaim)_2]^+$/$[Fe(salapy)_2]^+$ (FeN_4O_2), it is revealed that substitution of one phenolate for one imidazole/pyridine nitrogen lowers the potential by ≈500/≈600 mV. There are few reports on the electrochemical behaviour of high-spin iron(III) Schiff-base complexes.[32] This is the first time that a systematic study has been made on the Fe^{III}–Fe^{II} redox potentials for a closely related group of Schiff-base iron(III) complexes.

Relationship between Fe^{III}–Fe^{II} Redox Potential and Phenolate-to-iron(III) Charge-transfer Transition Energy.—With the present results we now have at hand Fe^{III}–Fe^{II} redox potentials and the lowest-energy l.m.c.t. band energies for a closely related group of six-co-ordinate high-spin iron(III) complexes.

The ligand-field potential[33] is made up of a spherical part and a directional part characteristic of the geometry of the complex. Compared to the directional potential which is responsible for the splitting of d orbitals, the spherical part is by far the most important contributor to the total energy and is repulsive in nature.[33] Qualitatively, one can predict that the spherical part[33] (V_s) should be sensitive to changes in the basicity of the ligand donor atoms, *i.e.* a more basic donor atom will increase V_s while a less basic group will decrease V_s. Thus, one would expect that the partially filled antibonding 'd' orbitals are higher in energy in a complex containing more basic donor atoms than in a complex containing less basic donor atoms. This prediction is in line with the observed (Fig. 4) linear dependence between the Fe^{III}–Fe^{II} redox potentials and the phenolate-to-iron(III) charge-transfer band energies in the closely related group of complexes **1**, **3**, **4**, **6** and **7**. We have not included complex **2** in this correlation since it behaves very differently so far as the UV/VIS spectrum is concerned (see above). Complex **5** is also excluded since the co-ordination geometry around iron(III) as well as the neutral nature of this complex make it different from other high-spin compounds. The phenolate-to-iron(III) charge-transfer band is thus an indicator of the redox potential of the metal centre as predicted by Que and co-workers.[7c] The complexes chosen in this correlation contain a set of ligands of varying Lewis basicities and charge, while retaining similar co-ordination geometries. The known $E_{298}°$ and l.m.c.t. energy of the high-spin iron(III) complexes of 2-(*o*-hydroxyphenyl)-*N*-(2-*N*-salicylideneaminoethyl)glycine[6d] and bis(3-*o*-hydroxybenzylideneaminopropyl)methylamine[32] also fit smoothly into the spectroelectrochemical correlation of Fig. 4. This is a more general type of correlation than that obtained by Que and co-workers[7c] using the [Fe(salen)X] series.

The tyrosine-to-iron(III) charge-transfer band maximum for the transferrins/lactoferrin is 465 nm.[5] The linear plot in Fig. 4 predicts a potential of −0.87 V *vs.* SCE, *i.e.* −0.63 V *vs.* NHE (normal hydrogen electrode). The formal reduction potential for iron(III) transferrin is estimated[34] to be ≈ −0.31 V *vs.* NHE. Thus, our correlation obtained using synthetic inorganic complexes predicts a reduction potential ≈300 mV more negative than that of the protein. A very recent transferrin model compound[6f] exhibits a potential of ≈ −0.82 V *vs.* NHE. The more negative potential observed for the model complexes is presumably a consequence of such factors as variances in the relative permittivity of the solvent medium *versus* the protein active site, the presence of (bi) carbonate ion in the active site of the protein and the differing charges due to hydrophobicity/hydrophilicity. The absolute value of the redox potentials of the iron tyrosinate proteins are not important but the observed trend (see below) is really impressive. The visible spectral band maxima[5] for the proteins catechol 1,2-dioxygenase and protocatechuate 3,4-dioxygenase occur at 455 and 460 nm, respectively. Our regression line predicts potentials of −0.97 and −0.92 V *vs.* SCE, *i.e.* −0.73 and −0.68 V *vs.* NHE. This is in line with the proposal[5] that these two proteins utilize the iron(III) oxidation state solely in the catalytic cycle. In the case of 4-hydroxyphenylpyruvate dioxygenase (595 nm)[5] our line predicts a potential of 0.35 V *vs.* NHE. This comparatively high value corroborates the suggestions[5] that here a mechanism involving oxygen binding to the iron(II) centre and subsequent activation is most likely to be operative. It is worth noting that the metal binding sites are known[2,4c] for the proteins lactoferrin, serum transferrin and protocatechuate 3,4-dioxygenase from X-ray crystallography. The predicted protein redox potentials are in conformity with the known iron co-ordination sphere.

Conclusion

In order to allow meaningful comparisons of the spectral (UV/VIS and EPR) and electrochemical properties for a group of high-spin octahedral iron(III) complexes, ligands were chosen in such a way that they belong to a common category, resulting in various co-ordination spheres, *viz.* FeN_4O_2, FeN_3O_3, $FeN_2O_2O'_2$, and FeN_2O_4. The absorption and EPR spectral properties of the complex $[Fe(salala)_2]^-$ are close to those of transferrins. From a study of the electrochemical behaviour of these complexes we have demonstrated that the nature of the ligand donor atom plays a very important role in the relative stabilization of one oxidation state over another. A linear spectroelectrochemical correlation has been provided which has more general applicability than the salen-based series of Que and co-workers.[7c] Thus, our primary goal of providing useful generalizations regarding the iron co-ordination environment in a closely related group of high-spin octahedral complexes *vis-à-vis* a trend in the redox potentials of iron tyrosinate proteins has been achieved.

Acknowledgements

Financial assistance from the Department of Science and Technology, Government of India, New Delhi, and the Council of Scientific and Industrial Research, New Delhi, is gratefully acknowledged. We thank Mr. D. K. Kannaujia and Mr. N. Ahmed for EPR and solution magnetic susceptibility/microanalytical measurements, respectively. Special thanks are due to Professor M. V. George for being helpful in many ways.

References

1 L. Que, jun., *Coord. Chem. Rev.*, 1983, **50**, 73.
2 A. L. Roe, D. J. Schneider, R. J. Mayer, J. W. Pyrz, J. Widom and L. Que, jun., *J. Am. Chem. Soc.*, 1984, **106**, 1676; B. F. Anderson, H. M. Baker, E. J. Dodson, G. E. Norris, S. V. Rumball, J. M. Waters and E. N. Baker, *Proc. Natl. Acad. Sci. USA*, 1987, **84**, 1769; S. Bailey, R. W.

Evans, R. C. Garratt, B. Gorinsky, S. Hasnain, C. Horsburgh, H. Jhoti, P. F. Lindley, A. Mydin, R. Sarra and J. L. Watson, *Biochemistry*, 1988, **27**, 5804.
3 L. Que, jun., *Struct. Bonding (Berlin)*, 1980, **40**, 39; *J. Chem. Educ.*, 1985, **62**, 938.
4 J. W. Whittaker, J. D. Lipscomb, T. A. Kent and E. Münck, *J. Biol. Chem.*, 1984, **259**, 4466; D. H. Ohlendorf, J. D. Lipscomb and P. C. Weber, *Nature (London)*, 1988, **336**, 403.
5 F. C. Bradley, S. Lindstedt, J. D. Lipscomb, L. Que, jun., A. L. Roe and M. Rundgren, *J. Biol. Chem.*, 1986, **261**, 11693 and refs. therein.
6 (*a*) B. P. Gaber, V. Miskowski and T. G. Spiro, *J. Am. Chem. Soc.*, 1974, **96**, 6868; (*b*) E. W. Ainscough, A. M. Brodie, J. E. Plowman, K. L. Brown, A. W. Addison and A. R. Gainsford, *Inorg. Chem.*, 1980, **19**, 3655; (*c*) M. G. Patch, K. P. Simolo and C. J. Carrano, *Inorg. Chem.*, 1983, **22**, 2630; (*d*) C. J. Carrano, K. Spartalian, G. V. N. Appa Rao, V. L. Pecoraro and M. Sundaralingam, *J. Am. Chem. Soc.*, 1985, **107**, 1651; (*e*) C. J. Carrano, M. W. Carrano, K. Sharma, G. Backes and J. Sanders-Loehr, *Inorg. Chem.*, 1990, **29**, 1865; (*f*) M. R. McDevitt, A. W. Addison, E. Sinn and L. K. Thompson, *Inorg. Chem.*, 1990, **29**, 3425.
7 (*a*) R. H. Heistand, II, A. L. Roe and L. Que, jun., *Inorg. Chem.*, 1982, **21**, 676; (*b*) R. H. Heistand, II, R. B. Lauffer, E. Fikrig and L. Que, jun., *J. Am. Chem. Soc.*, 1982, **104**, 2789; (*c*) J. W. Pyrz, A. L. Roe, L. J. Stern and L. Que, jun., *J. Am. Chem. Soc.*, 1985, **107**, 614; (*d*) L. S. White, P. V. Nilsson, L. H. Pignolet and L. Que, jun., *J. Am Chem. Soc.*, 1984, **106**, 8312; (*e*) L. Que, jun., R. C. Kolanczyk and L. S. White, *J. Am. Chem. Soc.*, 1987, **109**, 5373; (*f*) D. D. Cox and L. Que, jun., *J. Am. Chem. Soc.*, 1988, **110**, 8085; (*g*) L. Casella, M. Gullotti, A. Pintar, L. Messori, A. Rockenbauer and M. Györ, *Inorg. Chem.*, 1987, **26**, 1031; (*h*) F. Lloret, M. Mollar, J. Moratal and J. Faus, *Inorg. Chim. Acta*, 1986, **124**, 67.
8 R. H. Holm, G. W. Everett, jun. and A. Chakravorty, *Prog. Inorg. Chem.*, 1966, **7**, 83.
9 R. N. Mukherjee, T. D. P. Stack and R. H. Holm, *J. Am. Chem. Soc.*, 1988, **110**, 1850; R. N. Mukherjee, A. J. Abrahamson, G. S. Patterson, T. D. P. Stack and R. H. Holm, *Inorg. Chem.*, 1988, **27**, 2137; B. S. Snyder, G. S. Patterson, A. J. Abrahamson and R. H. Holm, *J. Am. Chem. Soc.*, 1989, **111**, 5214; K. K. Surerus, E. Münck, B. S. Snyder and R. H. Holm, *J. Am. Chem. Soc.*, 1989, **111**, 5501.
10 (*a*) L. Que, jun., R. H. Heistand, II, R. Mayer and A. L. Roe, *Biochemistry*, 1980, **19**, 2588; (*b*) R. B. Lauffer, B. C. Antanaitis, P. Aisen and L. Que, jun., *J. Biol. Chem.*, 1983, **258**, 14212.
11 A. B. P. Lever, *Inorg. Chem.*, 1990, **29**, 1271 and refs. therein.
12 D. T. Sawyer and J. L. Roberts, jun., *Experimental Electrochemistry for Chemists*, Wiley, New York, 1974.
13 M. Ray, S. Mukerjee and R. N. Mukherjee, *J. Chem. Soc., Dalton Trans.*, 1990, 3635.
14 L. C. Raiford and E. P. Clark, *J. Am. Chem. Soc.*, 1923, **45**, 1738.
15 D. F. Evans, *J. Chem. Soc.*, 1959, 2003.
16 (*a*) W. Gerger, U. Mayer and V. Gutmann, *Monatsh. Chem.*, 1977, **108**, 417; (*b*) C. J. O'Connor, *Prog. Inorg. Chem.*, 1982, **29**, 203.
17 (*a*) M. Kishita, Y. Muto and M. Kubo, *Aust. J. Chem.*, 1957, **10**, 386; (*b*) A. W. Baker and A. T. Shulgin, *J. Am. Chem. Soc.*, 1959, **81**, 1523.
18 (*a*) J. A. Broomhead and D. J. Robinson, *Aust. J. Chem.*, 1968, **21**, 1365; (*b*) D. F. Cook, D. Cummins and E. D. McKenzie, *J. Chem. Soc., Dalton Trans.*, 1976, 1369; (*c*) A. Malek, G. C. Dey, A. Nasreen and T. A. Chowdhury, *Synth. React. Inorg. Met.-Org. Chem.*, 1979, **9**, 145.
19 M. L. Duran, A. Rodriguez, J. Romero and A. Sousa, *Synth. React. Inorg. Met.-Org. Chem.*, 1987, **17**, 681.
20 R. C. Burrows and J. C. Bailar, jun., *J. Am. Chem. Soc.*, 1966, **88**, 4150.
21 J. C. Davis, W.-J. Kung and B. A. Averill, *Inorg. Chem.*, 1986, **25**, 394.
22 R. W. Oehmke and J. C. Bailar, jun., *J. Inorg. Nucl. Chem.*, 1965, **27**, 2209.
23 W. J. Geary, *Coord. Chem. Rev.*, 1971, **7**, 81.
24 E. Sinn, P. G. Sim, E. V. Dose, M. F. Tweedle and L. J. Wilson, *J. Am. Chem. Soc.*, 1978, **100**, 3375; P. G. Sim, E. Sinn, R. H. Petty, C. L. Merrill and L. J. Wilson, *Inorg. Chem.*, 1981, **20**, 1213; N. A. Bailey, D. Cummins, E. D. McKenzie and J. M. Worthington, *Inorg. Chim. Acta*, 1981, **50**, 111; R. B. Lauffer, R. H. Heistand, II and L. Que, jun., *Inorg. Chem.*, 1983, **22**, 50; B. J. Kennedy, G. Brain, E. Horn, K. S. Murray and M. R. Snow, *Inorg. Chem.*, 1985, **24**, 1647; B. J. Kennedy, A. C. McGrath, K. S. Murray, B. W. Skelton and A. H. White, *Inorg. Chem.*, 1987, **26**, 483; Y. Nishida, K. Kino and S. Kida, *J. Chem. Soc., Dalton Trans.*, 1987, 1157; S. M. Gorun, G. C. Papaefthymiou, R. B. Frankel and S. J. Lippard, *J. Am. Chem. Soc.*, 1987, **109**, 4244; P. Gomez-Romero, E. H. Witten, W. M. Reiff, G. Backes, J. Sanders-Loehr and G. B. Jameson, *J. Am. Chem. Soc.*, 1989, **111**, 9039 and refs. therein; T. Mizuta, T. Yamamoto, K. Miyoshi and Y. Kushi, *Inorg. Chim. Acta*, 1990, **175**, 121 and refs. therein.
25 W. T. Oosterhuis, *Struct. Bonding (Berlin)*, 1974, **20**, 59.
26 E. W. Ainscough, A. M. Brodie, J. E. Plowman, S. J. Bloor, J. Sanders-Loehr and T. M. Loehr, *Biochemistry*, 1980, **19**, 4072.
27 H. J. Schugar, G. R. Rossman, C. G. Barraclough and H. B. Gray, *J. Am. Chem. Soc.*, 1972, **94**, 2683; R. C. Reem, J. M. McCormick, D. E. Richardson, F. J. Devlin, P. J. Stephens, R. L. Musselman and E. I. Solomon, *J. Am. Chem. Soc.*, 1989, **111**, 4688.
28 C. R. Johnson, W. W. Henderson and R. E. Shepherd, *Inorg. Chem.*, 1984, **23**, 2754.
29 G. Ackerman and D. Hesse, *Z. Anorg. Allg. Chem.*, 1970, **375**, 77.
30 K. S. Schoefield, *Hetero-Aromatic Nitrogen Compounds*, Plenum, New York, 1967, p. 146.
31 N. S. Hush and R. J. M. Hobbs, *Prog. Inorg. Chem.*, 1968, **10**, 259; J. Sanders-Loehr, T. M. Loehr, A. G. Mauk and H. B. Gray, *J. Am. Chem. Soc.*, 1980, **102**, 6992.
32 A. W. Addison and C. G. Wahlgren, *Inorg. Chim. Acta*, 1988, **147**, 61 and refs. therein.
33 R. L. Lintvedt and D. E. Fenton, *Inorg. Chem.*, 1980, **19**, 569 and refs. therein.
34 W. R. Harris, *J. Inorg. Biochem.*, 1986, **27**, 41.

Received 27*th March* 1991; *Paper* 1/01471D